Computers, Environment and Urban Systems 87 (2021) 101602

Contents lists available at ScienceDirect

Computers, Environment and Urban Systems

journal homepage: www.elsevier.com/locate/ceus

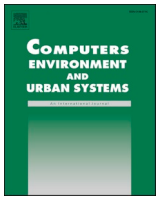

A multi-objective Markov Chain Monte Carlo cellular automata model: Simulating multi-density urban expansion in NYC

Ahmed Mustafa [a,*], Amr Ebaid [b], Hichem Omrani [c], Timon McPhearson [a,d,e]

[a] Urban Systems Lab, The New School, New York, USA
[b] Google LLC, California, USA
[c] Luxembourg Institute of Socio-Economic Research, Esch-sur-Alzette, Luxembourg
[d] Cary Institute of Ecosystem Studies, New York, USA
[e] Stockholm Resilience Centre, Stockholm, Sweden

ARTICLE INFO

Keywords:
Land use/cover change
Cellular automata
Optimization
Multi-objective Markov chain Monte Carlo
Multi-density urban

ABSTRACT

Cellular automata (CA) models have increasingly been used to simulate land use/cover changes (LUCC). Metaheuristic optimization algorithms such as particle swarm optimization (PSO) and genetic algorithm (GA) have been recently introduced into CA frameworks to generate more accurate simulations. Although Markov Chain Monte Carlo (MCMC) is simpler than PSO and GA, it is rarely used to calibrate CA models. In this article, we introduce a novel multi-chain multi-objective MCMC (mc-MO-MCMC) CA model to simulate LUCC. Unlike the classical MCMC, the proposed mc-MO-MCMC is a multiple chains method that imports crossover operation from classical evolutionary optimization algorithms. In each new chain, after the initial one, the crossover operator generates the initial solution. The selection of solutions to be crossed over are made according to their fitness score. In this paper, we chose the example of New York City (USA) to apply our model to simulate three conflicting objectives of changes from non-urban to low-, medium- or high-density urban between 2001 and 2016 using USA National Land Cover Database (NLCD). Elevation, slope, Euclidean distance to highways and local roads, population volume and average household income are used as LUCC causative factors. Furthermore, to demonstrate the efficiency of our proposed model, we compare it with the multi-objective genetic algorithm (MO-GA) and standard single-chain multi-objective MCMC (sc-MO-MCMC). Our results demonstrate that mc-MO-MCMC produces accurate simulations of land use dynamics featured by faster convergence to the Pareto frontier comparing to MO-GA and sc-MO-MCMC. The proposed multi-objective cellular automata model should efficiently help to simulate a trade-off among multiple and, possibly, conflicting land use change dynamics at once.

1. Introduction

Land use/cover change (LUCC) models are widely used in many applications such as understanding historical urbanization trends (e.g., Mustafa et al., 2018d), simulating urban development (e.g., Barreira-González, Aguilera-Benavente, & Gómez-Delgado, 2017; Omrani, Parmentier, Helbich, & Pijanowski, 2019), simulating agricultural systems (Xia et al., 2020), understanding the impacts of urban development on social segregation (e.g., Vermeiren, Vanmaercke, Beckers, & Van Rompaey, 2016), and on urban flooding (Chang, Lee, & Huang, 2017). Usually, LUCC dynamics involve multiple potentially conflicting objectives which requires trade-offs among these objectives. For instance, a grassland nearby an urban settlement will likely be developed to urban land. However, when we consider urban sub-uses, e.g., industrial, commercial, and residential, and/or sub-densities, e.g., high-, and low-density, this makes the problem very hard for urban planners to think about and assess all possibilities, especially considering that the LUCC process is complex involving many stakeholders, geophysical and socioeconomic aspects (Mustafa, Rompaey, Cools, Saadi, & Teller, 2018). One approach to examining the trade-off between different objectives is optimizing each objective in isolation and then formulating a large number of trial solutions delivered from the optimal "isolated" solutions (Dunnett et al., 2018). A major shortcoming of this approach is that it requires a considerable amount of time and it does not ensure that the

* Corresponding author.
E-mail addresses: a.mustafa@newschool.edu (A. Mustafa), amrebaid@google.com (A. Ebaid), hichem.omrani@liser.lu (H. Omrani), timon.mcphearson@newschool.edu (T. McPhearson).

https://doi.org/10.1016/j.compenvurbsys.2021.101602
Received 26 March 2020; Received in revised form 8 January 2021; Accepted 22 January 2021
Available online 13 February 2021

delivered multi-objective solution is the “near” optimal one. Often, the necessity for the multi-objective nature of the LUCC dynamic leads to the increased complexity of the process because neighboring and distant areas cannot be treated independently. In other words, spatial autocorrelation can bias the modeling’s results if objectives and constraints are not formulated carefully (Cao et al., 2011). Multinomial/binary logistic regression (logit) are static models that can address the spatial autocorrelation via a data sampling approach (Mustafa, Rompaey, et al., 2018; Puertas, Henríquez, & Meza, 2014). Although multinomial logit (MNL) models can measure the influence of various causative factors of LUCC related to accessibility, geophysical features, policies, and socioeconomic aspects, it is not recommended to incorporate local neighborhood settings into the MNL model as a static variable because the neighborhood settings are highly dynamic (Mustafa et al., 2018). A number of studies used search optimization algorithms such as genetic algorithms (GA) (e.g., García, Santé, Boullón, & Crecente, 2013; Mustafa et al., 2018) to calibrate neighborhood interactions in cellular automata (CA) models. Other search algorithms have been also used in the context of calibrating LUCC change models such as ant colony optimization (e.g., Ma, Li, & Cai, 2017), bee colony optimization (e.g., Yang, Tang, Cao, & Zhu, 2013), cuckoo search algorithm (e.g., Cao, Tang, Shen, & Wang, 2015), and particle swarm optimization (e.g., Feng et al., 2018).

Although Markov Chain Monte Carlo (MCMC) methods, such as Metropolis-Hastings and Simulated Annealing, have been used in optimization several decades ago (Geyer & Thompson, 1995; Hastings, 1970), they are rarely used to calibrate LUCC models. Al-Ahmadi, See, Heppenstall, and Hogg (2009) employed a single-objective simulated annealing algorithm to calibrate their CA model. They, furthermore, compared the performance of simulated annealing with GA and concluded that the GA produced a better calibrated model than simulated annealing. Vrugt, Gupta, Bastidas, Bouten, & Sorooshian, 2003 presented an extended MCMC method that considers multi-objective optimization of hydrologic models. This multi-objective MCMC (MO-MCMC) utilized the Pareto front concept that finds noninferior solutions in which an improvement in one objective requires a degradation in another. They concluded that the MO-MCMC has demonstrated effectiveness for finding the Pareto solutions.

MCMC is a stochastic optimization algorithm that uses sampling techniques for global optimization. At each iteration, the candidate state is accepted or rejected after comparing its fitness score to the previous score. With a sufficiently large number of samples, the algorithm guarantees the convergence of the sample distribution to the actual distribution. In contrast to MCMC, GA, the most common search algorithms used to calibrate multi-objective CA LUCC models (e.g., Cao et al., 2011; García, Rosas, García-Ferrer, & Barrios, 2017; Mustafa et al., 2018), is an evolutionary algorithm that starts by a random generation representing a population of the search space, and progressively selects random individuals to produce the children for the next generation using crossover and mutation operators, driving the population towards “near” optimal solution over successive generations. Machine learning (ML) methods are another way to calibrate LUCC model. Several studies demonstrated that ML-based methods outperform statistical calibration methods (e.g., Mileva, Suzana, Miloš, & Branislav, 2015; Mustafa et al., 2018). However, ML methods are not easily interpretable and are often used as black-boxes (Kuo, Huang, Zulvia, & Liao, 2018). Moreover, they require human supervision and pre-labeled training data, which might not always be feasible or affordable.

In this study, we introduce a novel MO-MCMC to calibrate a CA LUCC model. Al-Ahmadi et al. (2009) compared a single-objective MCMC algorithm with GA and found that GA outperformed MCMC. However, our hypothesis is that MCMC can achieve higher accuracy than GA as MCMC generates a larger number of "new" individual solutions comparing to GA and therefore explores more search spaces. Furthermore, MCMC would ensure faster convergence than GA by having multiple chains (different starts) and employing an exchange scheme between different chains. Our central question in this study is: Does multi-chain multi-objective MCMC improve CA model performance in terms of the accuracy of spatial allocation and computational time comparing to the most common algorithm used to calibrate multi-objective CA models (GA)?. To answer this question, we propose a novel CA LUCC model that efficiently combines multiple objectives. The model allocates LUCC over a geographic space according to a transition rule that consists of two distinct components. The first component measures the impact of a set of LUCC static causative factors (e.g., distance to roads, slope degree, etc.). The second component measures the impact of the dynamic neighborhood on each land unit. The first component is calibrated using the MNL model as in Mustafa et al. (2018b) and the second component is calibrated using MO-MCMC optimization. To our knowledge, no research exists within the LUCC modeling domain that introduces MO-MCMC in the LUCC model. Our MO-MCMC is based on the MCMC proposed by Gilks, Best, and Tan (1995) and the Metropolis–Hasting algorithm (Hastings, 1970; Metropolis, Rosenbluth, Rosenbluth, Teller, & Teller, 1953) and the more recent work of Li (2012). Our MO-MCMC has multiple chains (mc-MO-MCMC) and therefore reasonable samples may be obtained. A potential advantage of having multiple chains is the possible interaction between them. Our model stores all solutions proposed in each chain and therefore it is expected that the solutions hold useful information about the directions towards the optimal solution space. Thus, after the first chain, we use the genetic algorithm crossover operator to create the initial solution for each new chain. The acceptance rate is used to tune the solutions towards the Pareto optimal front with time. The objective function is the maximization of the agreement between the simulated map and the observed land-use/cover (LUC) map by means of fuzzy similarity.

The non-urban to low-, medium-, or high-density urban transitions in New York City (USA) between 2001 and 2016 were chosen as a case study application to demonstrate the applicability of our proposed model. Two observed LUC maps and six input variables related to geophysical, accessibility, socioeconomic aspects are used to calibrate the model. In order to highlight the potential of our mc-MO-MCMC CA model, we compare its performance with a CA model that is calibrated using multi-objective GA (MO-GA) and the classical single-chain MO-MCMC (sc-MO-MCMC).

The following sections describe our mc-MO-MCMC CA model framework, case study, experimental results, and then provide our conclusions and future research directions.

2. Model structure

LUCC model presented in this study consists of two distinct modules: demand and allocation. The demand module estimates the rate of change from one LUC state to another state each timestep. The allocation module allocates the required changes per timestep over the entire study area. The demand module can either calculate the change rates based on past observed trends or be fed with the expected quantity of changes. The allocation module is a CA raster-based model. Fig. 1 outlines the general framework of the proposed model.

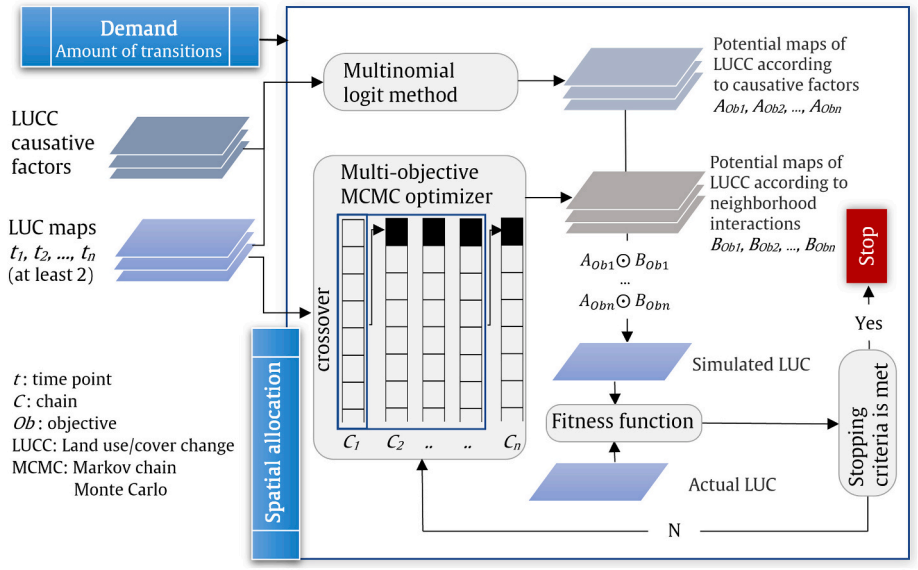

Fig. 1. Flowchart of the modeling land use/cover changes (LUCC) using multi-objective Markov Chain Monte Carlo (MCMC) Cellular Automata model.

2.1. Cellular automata land-use/cover change model

Cellular Automata (CA) is a bottom-up dynamic modeling approach that is widely used to model LUCC (Chen, Li, Liu, & Ai, 2014; Feng et al., 2018; Mustafa, Heppenstall, et al., 2018). The model is raster-based uses a multi-objective approach to allocate multiple changes simultaneously, e.g., changes from grasslands to urban, arable lands, and forests. Multi-objective allocation procedure is necessary as each LUC class has its own preference with respect to compatibility with a neighborhood of different LUC classes. The spatial LUC transition potential P of a cell i,j being change its current LUC state at a certain timestep can be determined by the following equation:

$$P_{i,j} = (P_n)_{i,j} \times (P_c)^{\alpha}_{i,j} \times (P_{con})_{i,j} \quad (1)$$

where $(P_n)_{i,j}$ is the local neighborhood (endogenous) effect on this cell, $(P_c)_{i,j}$ is the potential of LUCC according to (exogenous) causative factors, α is a parameter expresses the importance of the causative factors, and $(P_{con})_{i,j}$ is the restrictive conditions for LUCC. The $(P_c)_{i,j}$ is produced by a non-binary logistic regression. The model performs the proportional odds assumption test (Kim, 2003) to opt for ordered or non-ordered multinomial logistic regression (MNL). Prior to running the MNL, the variance inflation factors (VIF) test is performed to measure the multicollinearity to ensure that there are no two or more causative factors measuring the same phenomena. The model, therefore, excludes factors that have VIF > 4 (Montgomery & Runger, 2003). This exclusion is an iterative procedure, i.e., the model excludes one variable at a time and reperforms the VIF test, and repeats until all variables have VIF ≤ 4. Because because the causative factors are measured in different units, e.g., meters, percentages, etc., the model standardizes all factors. Furthermore, the model employs a data sampling approach to address the spatial autocorrelation phenomena that may bias the results of the regression analysis (Mustafa, Heppenstall, et al., 2018; Rienow & Goetzke, 2015).

2.1.1. Multi-objective Markov Chain Monte Carlo

In our model, the local neighborhood effect $(P_n)_{i,j}$ represents a square space D, the Moore neighborhood, around the central cell and contains a number of cells that are arranged in a determined number of square distance zones d. The $(P_n)_{i,j}$ is calculated in each timestep according to the procedure of White and Engelen (2000) as follows:

$$(P_n)_{i,j} = \Sigma_l \Sigma_d w_{kd} \quad (2)$$

where w_{kd} is the weighting parameter assigned to a cell I,j with LUC class k at distance zone d of the neighborhood D. The weighting parameters that define the neighborhood's attraction or repulsion for LUC k are automatically calibrated by multi-chains multi-objective Markov Chain Monte Carlo (mc-MO-MCMC). The mc-MO-MCMC objective is to find the parameters that achieve the highest allocation accuracy rate for the process of changing LUC k to other classes (for example, transitions from forest to low-, medium-, high-density urban, grassland, or arable land simultaneously).

The mc-MO-MCMC seeks a parameter vector v that yields the pareto front PF solution by attempting a number of states n changes according to a proposed solution. Each solution is proposed by a sampling procedure that generates random numbers from the continuous uniform distributions with lower and upper endpoints. The acceptance probability of changing the last accepted state st, for $t \in [1,n]$, to a new state V is determined by the Metropolis–Hastings rule ω (Hastings, 1970; Metropolis et al., 1953). In our model, the ω is calculated as follows:

$$\omega = min\left(1, e^{\left(fit\left(\frac{v}{100}\right) - fit\left(\frac{st}{100}\right)\right)^t}\right) \quad (3)$$

where $fit()$ is the fitness score assigned to a solution vector V according to the fitness function. The proposed solution is then accepted with the probability $\xi \leq \omega$ *accept* V (4) where ξ is a uniform random number between 0 and 1. The t, Eq. 3, that is increased with an increase in the number of stats, is used to control the acceptance rate over time. Lower t, at the beginning of each chain, allows the mc-MO-MCMC sampler to explore solutions far away from the Pareto front space in order to discover more search spaces whilst a higher t helps the sampler to converge towards the optimal solution by the end of the chain C. The number of chains is not predefined. Instead, the model uses a convergence stopping criterion when the fitness score for 10 successive chains becomes similar ($\Delta < 0.001$).

The key feature of our mc-MO-MCMC is that it considers multiple vertical chains. Although in literature, there is a great interest in parallel implementation of MCMC algorithms (e.g., Scott et al., 2016; Strid, 2010) to reduce the computing time, our goal here is to improve the overall performance of the LUCC models. The mc-MO-MCMC proposed here applies an exchange scheme by crossing over a certain number of available solutions selected according to their fitness scores. The outcome "crossed over" solution represents an adaptive function to

Pseudo Code of mc-MO-MCMC

```
PF ← ∅                                                  //Pareto front solution
S ← ∅                                                   //Set of all solutions
C ← 1                                                   //Chains

while stopping criterion not met:                       //delta < 0.001
  for t = 1 to n:                                       //n timesteps
      V ← RandomVector(N)                               //N objectives in V
    if t == 1:
      if C > 1:
       V ← EliteCrossover(S)                            //Elite vector
      end if
      st ← V                                            //Last accepted state
    end if
    S.append(V)
    if F(O1) >= F(O*1)... and F(ON) >= F(O*N)
      PF ← V                                            //Improved objective(s)
    end if
    w ← MetropolisHastings(V, st, t)
    e ← Random(0, 1)
    if e <= w:
      st ← V
    end if                                              //Accept candidate
  end for
  C ← C + 1
end while
```

Fig. 2. The mc-MO-MCMC.

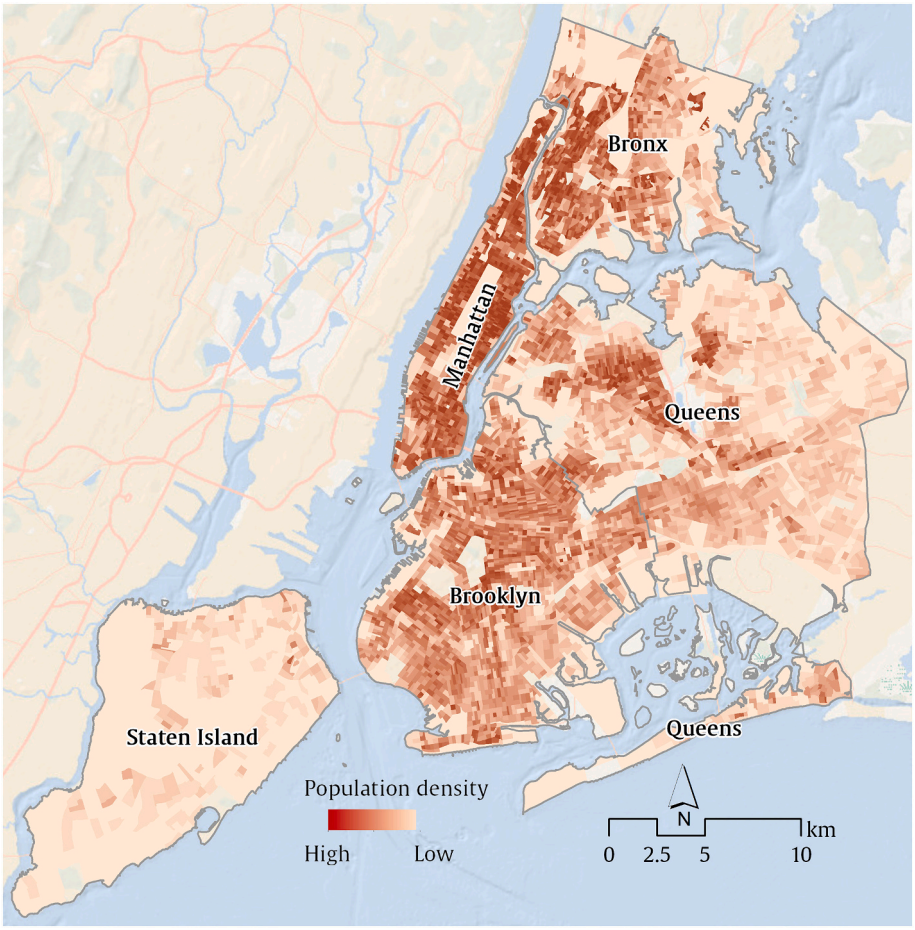

Fig. 3. Population density in New York City (2018 American Community Survey).

guide the search to more precise jumps and thus results in a faster MCMC convergence. In our model, the crossover occurs considering the whole population of performed chains to take advantage of the available information, directions and distances, of all explored areas within the search space. The number of solutions selected, parents, to be crossed over and to create the initial solution for the next chain is equal to the number of objectives O_N being searched. The model selects the best vectors that represent one objective from each parent. One can claim that this elitist selection process may cause the premature convergence of the algorithm. However, lower t values, Eq. (3), at the beginning of each chain helps to prevent mc-MO-MCMC from early convergence. Fig. 2 presents the Pseudo Code of the proposed mc-MO-MCMC.

2.1.2. Model evaluation and fitness function

The proposed model solves multi-objective land allocation problems by determining a compromise noninferior solution in which an improvement in one objective requires a degradation in another. The fitness function used to evaluate the model's allocation ability is the maximization of the fuzziness similarity rate between simulated and observed maps. The fitness function considers only new LUC changes to avoid having a high allocation accuracy rate which is a result of the persistence of unchanged cells within the study period. The fuzziness similarity rate (FSR) is calculated for each equally important objective as follows (Mustafa, Heppenstall, et al., 2018):

$$FSR_k = \frac{\sum_{x_k \in X_{k,sim}} \left| I_{x_k 0} \cdot (1/2)^{0/2}, I_{x_k 1} \cdot (1/2)^{1/2}, \ldots\ldots, I_{x_k d} \cdot (1/2)^{d/2} \right|_{\max}}{X_{k,actul}} \times 100 \quad (5)$$

where FSR_k ($0 \leq FSR_k \leq 100$) is the fuzziness similarity rate for LUC class k, I_{ikd} is 1 if cell i_k in the simulated map at zone d ($0 \leq d \leq 4$) has the similar k to one cell at zone d in the observed map otherwise is 0, $X_{k,sim}$ is the total changes of k in the simulated map and $X_{k,actul}$ is the total changes of k in the observed map. Comparing to spatial overlay tthat adopts a cell to cell location agreement, an advantage of a fuzzy similarity method (Hagen, 2003) is that it can differentiate between near and far misses as they operate at larger scales than the cell.

3. Case study and results

To evaluate the performance of the proposed mc-MO-MCMC CA model, we applied it to simulate urban expansion of three different densities, objectives, in New York City (USA) between 2001 and 2016. Furthermore, we applied two other models: MO-GA CA and sc-MO-MCMC CA and compared them with the mc-MO-MCMC CA.

3.1. Study area

New York City (NYC) is the most populous and densest US city with more than 8.4 million people according to the 2018 American Community Survey. It is located on the coast of the Northeastern United States and covers ~784 km^2. NYC is made up of five county-level administrative divisions or "boroughs": The Bronx, Brooklyn, Manhattan, Queens, and Staten Island. The population is highly concentrated in Manhattan and Brooklyn (Fig. 3). The city lies at the confluence of several rivers and the majority of the Metropolitan region situated less than 5 m above the mean sea level (Colle et al., 2008). The number of 30 × 30 m cells that changed their state from non-urban to low-density, medium-density, and high-density (our three objectives) between 2001 and 2016 were 7704, 6946, and 2398 respectively. Various rates of changes are important to demonstrate the spatial allocation ability of the LUCC model, particularly low rates, such as non-urban to high-density urban in our case study, because low change rate means having less information to calibrate/train any model.

Table 1
The aggregated nine land use/cover classes used in this study.

Original NLCD classes		Aggregated classes	
Class code	Description	Class code	Description
11	Open Water	9	Water
12	Perennial Ice/Snow	9	Water
21	Developed, Open Space	4	Built-up Open/Green
22	Developed, Low Intensity	1	Built-up Low-density
23	Developed, Medium Intensity	2	Built-up Med-density
24	Developed High Intensity	3	Built-up High-density
31	Barren Land	5	Grasslands/Barren Lands
41	Deciduous Forest	7	Forests
42	Evergreen Forest	7	Forests
43	Mixed Forest	7	Forests
51	Dwarf Scrub	7	Forests
52	Shrub/Scrub	7	Forests
71	Grassland/Herbaceous	5	Grasslands/Barren Lands
72	Sedge/Herbaceous	5	Grasslands/Barren Lands
73	Lichens	5	Grasslands/Barren Lands
74	Moss	5	Grasslands/Barren Lands
81	Pasture/Hay	6	Cultivated lands
82	Cultivated Crops	6	Cultivated lands
90	Woody Wetlands	8	Wetlands
95	Emergent Herbaceous Wetlands	8	Wetlands

3.2. Data

Primary datasets in this case study are two observed LUC maps and associated LUCC causative factors. Two LUC maps for 2001 and 2016 were extracted from United States National Land Cover Database (NLCD) that is a raster dataset at 30-m spatial resolution (Homer et al., 2007; Yang et al., 2018). Because the NLCD team follows strict image classification and post-classification procedures, the produced LUC information tends to be accurate and consistent. Yang et al. (2018) reported that the overall agreement of NLCD is 90% for 2001 and 88% for 2016. The original NLCD 20 classes were grouped into nine aggregated LUC classes (Table 1): 1 Built-up low-density, 2 Built-up medium-density, 3 Built-up high-density, 4 Built-up open/green spaces, 5 Grasslands/barren lands, 6 Cultivated lands, 7 Forests, 8 Wetlands, and 9 Water bodies. The built-up density represents percent imperviousness which considers a cell with impervious surfaces accounting for 20% to 49% as low-density, 50% to 79% as medium-density, and 80% to 100% as high-density. A series of geophysical and socioeconomic factors were introduced as LUCC causative factors in this case study, Fig. 4. Elevation and slope (geophysical factors) were derived from United States Geological Survey (USGS) 10- and 30-m Digital Elevation Models (DEMs). Euclidean distances to highways and local roads (accessibility factors) were extracted from USGS National Transportation Dataset (NTD) that was published in September 2019. Total population and total households' income (socioeconomic factors) were delivered from American Community Survey (ACS) of 2016. All the input data were generated at or resampled to 30-m spatial resolution to meet the NLCD data resolution.

3.3. Model configurations

The model is calibrated based on the observed changes from non-urban to one of the urban densities (low, medium, or high) between 2001 and 2016. The model's performance (Eq. (5)) is calculated by comparing the simulated map of 2016 with the observed 2016 map. For this case study, the quantity of change equals the observed number of new urban cells for the study period divided by timesteps. The temporal

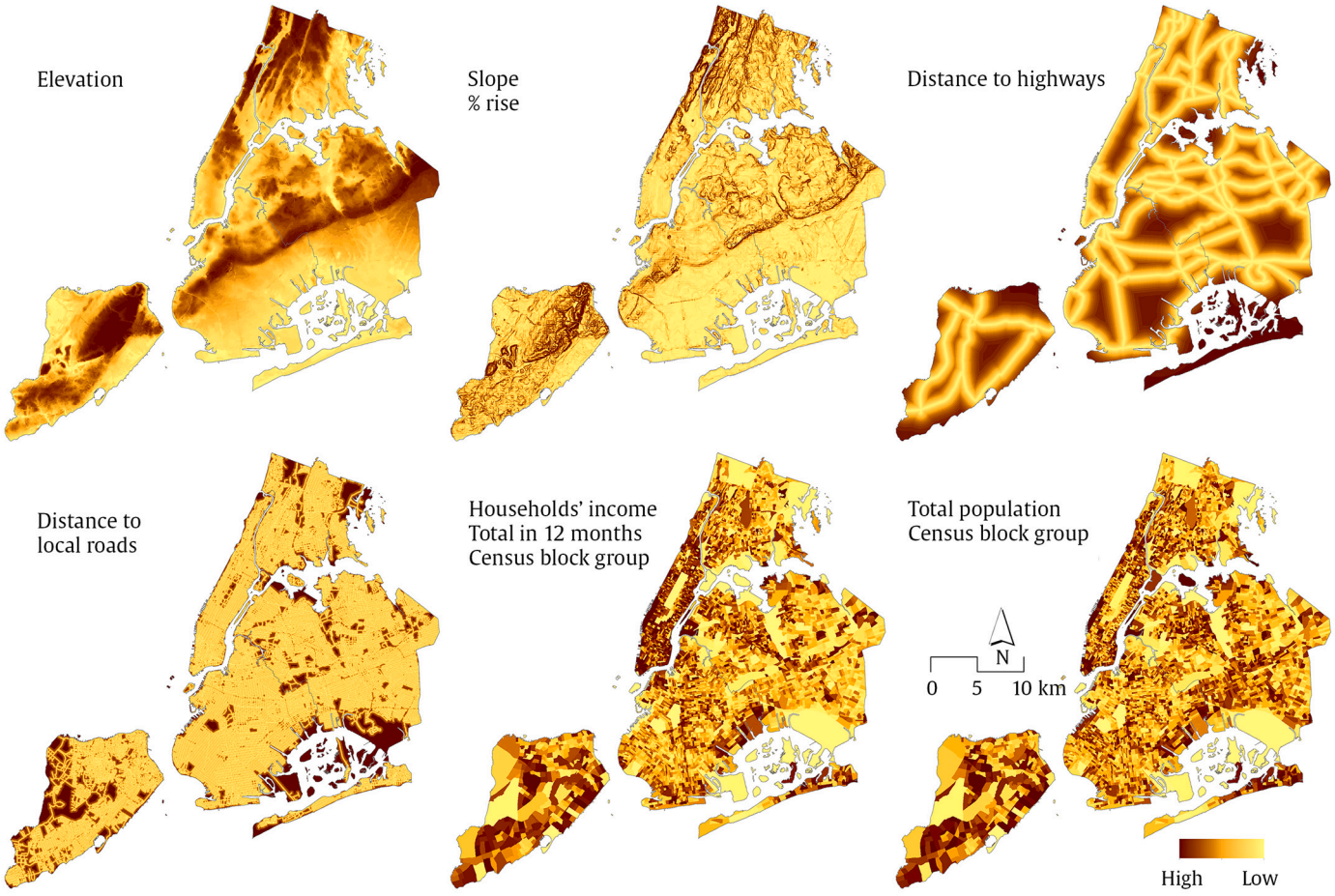

Fig. 4. Land use/cover change causative factors for New York City case study.

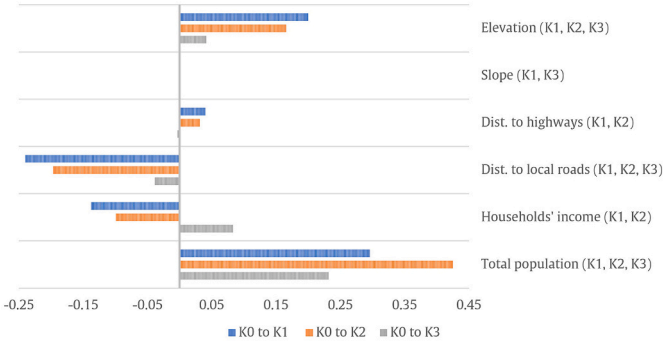

Fig. 5. MNL causative factors coefficients and significance level p-value ≤ 0.05 (in brackets).

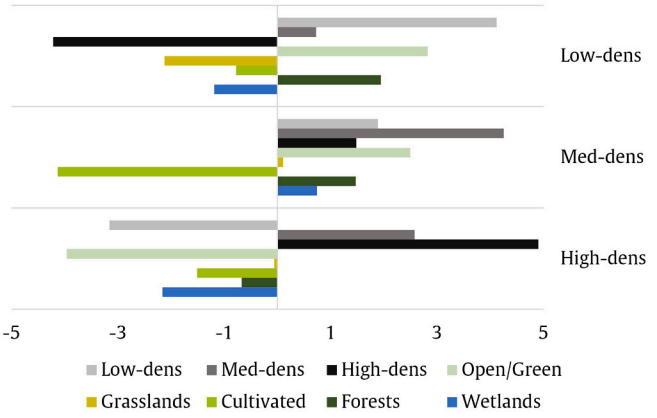

Fig. 6. Weighting parameters (y-axis) that represent the interaction between an urban cell with a certain density and other LUC.

resolution (timestep) for our case study is set at one year. We did not set any constraints so the $(P_{con})_{i,j}$ in Eq. (1) is 1. The neighborhood (Eq. (2)) size is 3 × 3 neighborhood window. The selection of the window size is made based on the findings of previous studies (Chen et al., 2014; Mustafa, Rienow, et al., 2018) that conducted a comprehensive sensitivity analysis to identify the best neighborhood window size. Chen et al. (2014) used the same a spatial resolution of 30-m as our case study.

The significance of the chi-squared statistic of the proportional odds assumption is <0.001 so that the assumption of having a natural ordering in the dependent variable is violated. Consequently, the model employs a non-ordered multinomial logistic regression (MNL) to calculate the $(P_c)_{i,j}$ in Eq. (1) according to Mustafa et al., 2018. The main theme of this paper is the calculation of $(P_n)_{i,j}$ in Eq. (2) that is calculated using our novel mc-MO-MCMC. As GA are well known method to solving multi-objective optimization problems (Cao et al., 2011; XIU, 2000), we also calculated $(P_n)_{i,j}$ using MO-GA and compared the results with the mc-MO-MCMC. The various MO-GA operators (selection, crossover, and mutation) were determined by undertaking empirical experiments on several values with low number of generations as in Mustafa et al., 2018. The best performing operators' settings will then used in the final MO-GA runs. We also tested several numbers of chains and solutions per chain for mc-MO-MCMC.

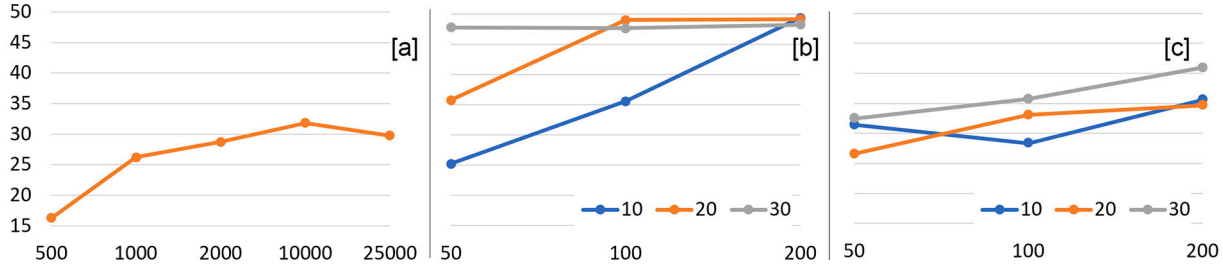

Fig. 7. The average FSR (y-axis) for number of solutions (x-axis) for (a) sc-MO-MCMC, (b) mc-MO-MCMC (with 10, 20 and 30 chains), and (c) MO-GA (with 10, 20 and 30 generations).

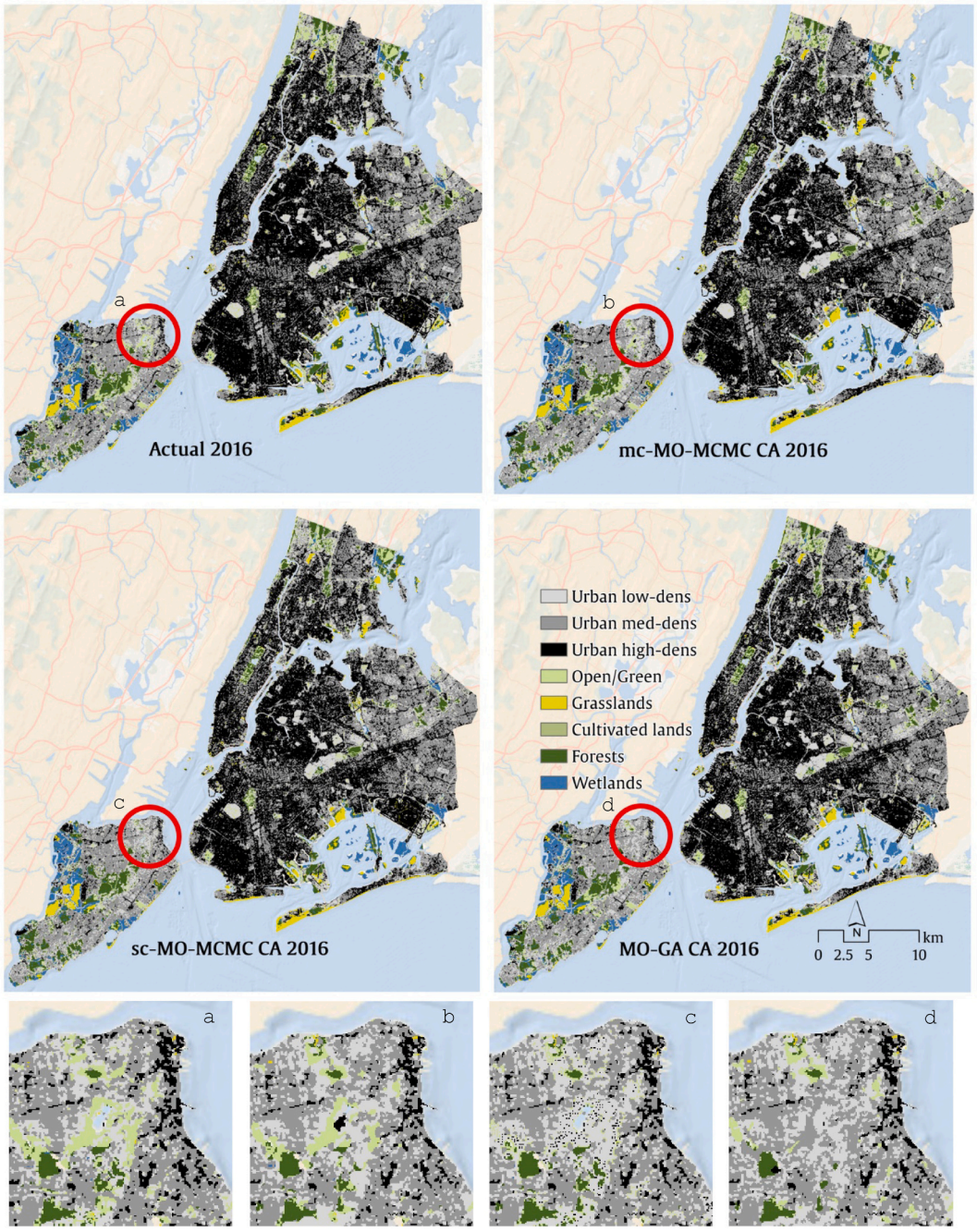

Fig. 8. Comparison of observed and simulated maps for 2016 generated by different models in study area.

Table 2
The FSR (%) for the best pareto front solutions for each model.

	k0 to k1	k0 to k2	k0 to k3	average	σ*
mc-MO-MCMC**	50.60	49.66	47.07	49.11	1.49
sc-MO-MCMC***	38.15	49.67	7.73	31.85	17.69
MO-GA****	42.72	32.61	47.46	40.93	6.19

* Standard deviation.
** Number of chains: 20; solutions per chain: 200 (total solutions: 4000).
*** Number of solutions: 10,000 (total solutions: 10,000).
**** Number of generations: 30; solutions per generation: 200 (total solutions: 6000).

3.4. Results and discussions

Our model has been coded in MATLAB and run on a PC clocked at 2.60 GHz with a 32.0 GB RAM. The proposed mc-MO-MCMC CA stopped after 33 chains (with 200 solutions per chain) and reached an average FSR (Eq. (5)) of 49.7. The results of multinomial logistic regression (MNL) (Fig. 5) show that elevation, Euclidean distance to local roads, and total population are the only factors that are statistically significant in all changes (from non-urban K0 to low-density K1, medium-density K2, and high-density urban K3). By far, total population is the most dominant factor. Interestingly, average household income shows an inverse significant correlation with low- and medium-density development implying that rich people tend to live in lower-density districts. The inverse correlation between distance to local roads and urban development indicates that new urban development especially low- and medium-density are likely to happen near local roads.

The weights calibrated by the mc-MO-MCMC that defines the neighborhood interactions are presented in Fig. 6. The calibration finds a remarkable positive correlation between the development of new low-density urban areas and the number of existing low-density urban lands within the neighborhood. Furthermore, it is notable that low-density development is most likely found away from high-density urban areas and near urban green areas and forests. In contrast, the potential of finding new high-density projects is increased near or within high-

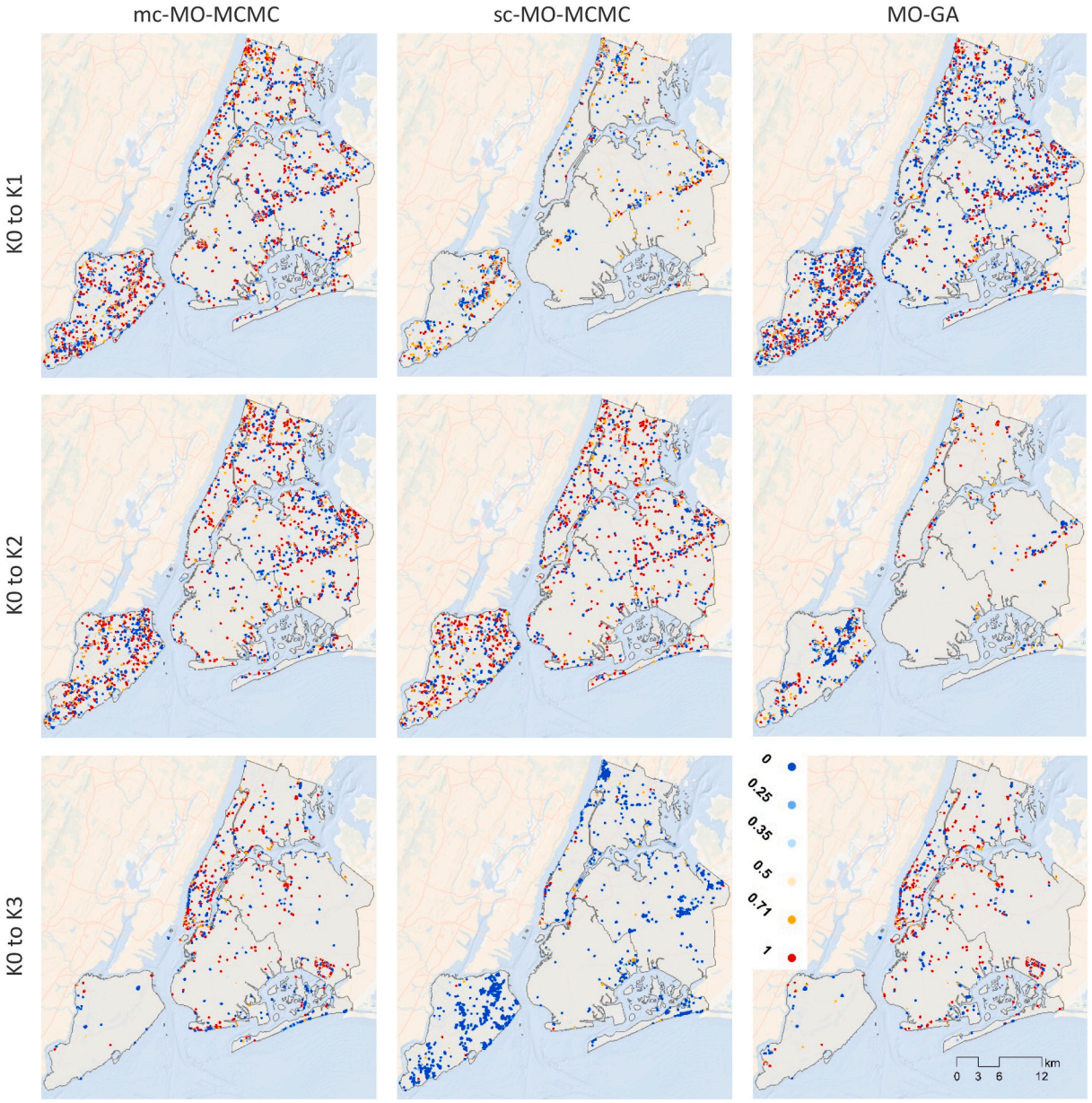

Fig. 9. The fuzzy similarity rate (FSR) of the newly allocated cells. FSR ranges from 1 (if the model allocated the cell in the correct location) to 0 (if the cell was allocated more than four cells away from the correct location).

Table 3
The percentage of new cells (% of total changes) within each fuzzy similarity rate (FSR) for each objective (from non-urban k0 to low-dens k1, medium-dens k2, or high-density urban k3).

FSR	K0 to K1			K0 to K2			K0 to K3		
	mc-MO-MCMC	sc-MO-MCMC	MO-GA	mc-MO-MCMC	sc-MO-MCMC	MO-GA	mc-MO-MCMC	sc-MO-MCMC	MO-GA
0	22.25	26.61	31.66	27.03	26.11	41.08	35.51	86.37	34.55
0.25	9.49	14.10	9.64	7.65	7.43	11.30	5.53	2.98	5.91
0.35	11.46	15.97	12.06	8.61	9.46	12.30	6.42	2.10	7.21
0.5	14.07	17.86	13.71	13.07	13.87	12.30	9.27	2.68	9.60
0.71	19.13	18.47	14.24	18.76	19.19	13.32	15.39	3.31	14.88
1	23.60	6.99	18.69	24.88	23.95	9.70	27.88	2.56	27.84

density urban neighborhoods and when being away from low-density neighborhoods. The calibration also shows that new medium-density urban developments are positively influenced by the existing medium-density lands and negatively by cultivated lands. The relative importance of the causative factors α (Eq. (1)) is 0.06, 0.28, and 0.16 for low-density, medium-density, and high-density developments respectively implying that neighborhood effect has a greater influence on all types of urban developments than the selected causative factors (Section 3.2).

The run time of the three models is slightly different. The average run time per 100 solutions are 872, 861, and 880 s for the mc-MO-MCMC CA, sc-MO-MCMC CA, and MO-GA CA respectively. The reason is that the single chain MO-MCMC has less operators (acceptance rate) than multi-chain MO-MCMC (acceptance rate, selection, and crossover) and MO-GA (selection, crossover, and mutation operators).

Fig. 7 illustrates the average FSR for the best Pareto front solution for the three models using different sets of the number of chains/generations and a number of solutions. For the sake of comparison, we predefined the number of chains/generations and individual solutions per chain/generation for MCMC and GA. The multiple graphs reveal that our mc-MO-MCMC CA model approaches the "near" optimal search space in much fewer iterations than MO-GA and with much fewer solutions than MO-GA and sc-MO-MCMC, which clearly indicates that the proposed model performs much better than other models in terms of computation time (lower number of runs) and allocation accuracy. This can be explained by the fact that the proposed model takes more adaptive moves by exploring the distance between and direction of all available solutions.

Fig. 8 shows the actual LUC map of 2016 and the 2016 maps simulated by different models. The simulated map generated by the mc-MO-MCMC CA model matches better the actual 2016 map compared to other models. Table 2 lists the best pareto front FSR for each objective (changes from non-urban K0 to low-density K1, medium-density K2, and high-density urban K3). The findings indicate that the proposed mc-MO-MCMC provides a good trade-off between objectives.

The detailed FSR is shown in Fig. 9. This figure demonstrates the allocation ability of the mc-MO-MCMC CA model to properly allocate the new cells over the study area. Table 3 lists the number of allocated cells in each FSR class. These FSR classes resulted from the fuzzy membership function of exponential decay with a halving distance of two cells and a neighborhood window of four cells (Eq. 5). The model spatially allocates 42.7%, 43.6%, and 43.3% of the new cells of low-density, med-density, and high-density respectively, at the correct location or at the adjacent cell which is significantly better than sc-MO-MCMC and MO-GA.

Both MCMC and GA are stochastic optimizers that start from a random search with no prior information. Thus, the variability of the modeling outputs is a crucial aspect to be addressed. For instance, we ran our mc-MO-MCMC model 10 times, each run had 10 chains and each chain had 200 individual solutions. The average Kappa index that expresses the spatial agreement among the 10 simulations is 0.63 (1 indicates a maximum level of agreement) considering only the new urban cells. In our case study, we tested several runs with various numbers of chains and solutions per chain. Our results (Fig. 6) represent the best model run. An alternative approach to address the variability of the modeling outputs is to have multiple runs and assign a probability value for each land unit, e.g., cell, that represents the frequency at which the model changed the cell's LUC state (Rienow & Goetzke, 2015).

4. Conclusions and future work

The objective of this study was to explore the potential of using a multi-objective Markov Chain Monte Carlo (MO-MCMC) to calibrate land-use/cover change (LUCC) models that consider multiple allocation objectives. We developed a raster-based cellular automata (CA) model to present and evaluate the proposed MO-MCMC calibration method. We compared our CA model with a model that has been calibrated using a multi-objective genetic algorithm (MO-GA) because the MO-GA is one of the most employed algorithms to calibrate multi-objective LUCC models. With three simultaneous objectives, our case study in New York City clearly demonstrated the potential of our model to simulate LUCC dynamics more accurately and faster than the MO-GA. It worth mentioning that the proposed model can simulate the full LUCC transitions between all nine LUC classes (Table 1). However, our focus in this article was on introducing the novel mc-MO-MCMC CA model and comparing it with MO-GA CA.

Although the focus of this study was on only three objectives, the results showed the potential of the model for handling many objectives and variables. In this sense, one of the important directions for future research is to extend our model to handle LUCC practices that seek a trade-off between multiple physical and social concerns. This is especially important for strategies that address multiple domains (e.g., Iwaniec et al., 2020; Keeler et al., 2019), and therefore our model can bring analytical and simulation approaches in the planning process in which planners and various stockholders need to reveal the tensions between plausibility and desirability in future LUCC visions. For example, as a multi-objective model, our model could simulate the trade-off between different LUCC visions that promote either economic welfare, social equity, or environmental protection objective. Future work should also explore the effects of spatial heterogeneity, and examine the models' sensitivity related to uncertainty and neighborhood size. Lastly, the development of a generic LUCC tool with a user interface is the final goal of this research.

Software and data availability

All data used in this case study are publicly provided by USGS https://viewer.nationalmap.gov/basic/ and US Census Bureau https://www.census.gov/programs-surveys/acs/guidance/comparing-acs-data/2016.html. MATLAB codes of the developed model are available upon reasonable request from the corresponding author.

Acknowledgement

This material was supported by US National Science Foundation "GCR: Social, Ecological, and Technological Infrastructure Systems for Urban Resilience" (Award #1934933) and "Urban resilience to extreme

weather related events" (Award #1444755) projects.

References

Al-Ahmadi, K., See, L., Heppenstall, A., & Hogg, J. (2009). Calibration of a fuzzy cellular automata model of urban dynamics in Saudi Arabia. *Ecological Complexity, 6*, 80–101. https://doi.org/10.1016/j.ecocom.2008.09.004.

Barreira-González, P., Aguilera-Benavente, F., & Gómez-Delgado, M. (2017). Implementation and calibration of a new irregular cellular automata-based model for local urban growth simulation: The MUGICA model. *Environment and Planning B-Urban Analytics and City Science*. https://doi.org/10.1177/2399808317709280, 2399808317709280.

Cao, K., Batty, M., Huang, B., Liu, Y., Yu, L., & Chen, J. (2011). Spatial multi-objective land use optimization: Extensions to the non-dominated sorting genetic algorithm-II. *International Journal of Geographical Information Science, 25*, 1949–1969. https://doi.org/10.1080/13658816.2011.570269.

Cao, M., Tang, G., Shen, Q., & Wang, Y. (2015). A new discovery of transition rules for cellular automata by using cuckoo search algorithm. *International Journal of Geographical Information Science, 29*, 806–824. https://doi.org/10.1080/13658816.2014.999245.

Chang, Y.-T., Lee, Y.-C., & Huang, S.-L. (2017). Integrated spatial ecosystem model for simulating land use change and assessing vulnerability to flooding. *Ecological Modelling, 362*, 87–100. https://doi.org/10.1016/j.ecolmodel.2017.08.013.

Chen, Y., Li, X., Liu, X., & Ai, B. (2014). Modeling urban land-use dynamics in a fast developing city using the modified logistic cellular automaton with a patch-based simulation strategy. *International Journal of Geographical Information Science, 28*, 234–255. https://doi.org/10.1080/13658816.2013.831868.

Colle, B. A., Buonaiuto, F., Bowman, M. J., Wilson, R. E., Flood, R., Hunter, R., … Hill, D. (2008). New York City's vulnerability to coastal flooding. *Bulletin of the American Meteorological Society, 89*, 829–842. https://doi.org/10.1175/2007BAMS2401.1.

Dunnett, A., Shirsath, P. B., Aggarwal, P. K., Thornton, P., Joshi, P. K., Pal, B. D., … Ghosh, J. (2018). Multi-objective land use allocation modelling for prioritizing climate-smart agricultural interventions. *Ecological Modelling, 381*, 23–35. https://doi.org/10.1016/j.ecolmodel.2018.04.008.

Feng, Y., Wang, J., Tong, X., Liu, Y., Lei, Z., Gao, C., & Chen, S. (2018). The effect of observation scale on urban growth simulation using particle swarm optimization-based CA models. *Sustainability, 10*, 4002. https://doi.org/10.3390/su10114002.

García, A. M., Santé, I., Boullón, M., & Crecente, R. (2013). Calibration of an urban cellular automaton model by using statistical techniques and a genetic algorithm. Application to a small urban settlement of NW Spain. *International Journal of Geographical Information Science, 27*, 1593–1611. https://doi.org/10.1080/13658816.2012.762454.

García, G. A., Rosas, E. P., García-Ferrer, A., & Barrios, P. M. (2017). Multi-objective spatial optimization: Sustainable land use allocation at sub-regional scale. *Sustainability, 9*, 927. https://doi.org/10.3390/su9060927.

Geyer, C. J., & Thompson, E. A. (1995). Annealing Markov chain Monte Carlo with applications to ancestral inference. *Journal of the American Statistical Association, 90*, 909–920. https://doi.org/10.2307/2291325.

Gilks, W. R., Best, N. G., & Tan, K. K. C. (1995). Adaptive rejection Metropolis sampling within Gibbs sampling. *Journal of the Royal Statistical Society. Series C, Applied Statistics, 44*, 455–472. https://doi.org/10.2307/2986138.

Hagen, A. (2003). Fuzzy set approach to assessing similarity of categorical maps. *International Journal of Geographical Information Science, 17*, 235–249. https://doi.org/10.1080/13658810210157822.

Hastings, W. K. (1970). Monte Carlo sampling methods using Markov chains and their applications. *Biometrika, 57*, 97–109. https://doi.org/10.2307/2334940.

Homer, C. G., Dewitz, J., Fry, J., Coan, M., Hossain, N., Larson, C., … Wickham, J. (2007). Completion of the 2001 National Land Cover Database for the conterminous United States. *Photogrammetric Engineering and Remote Sensing, 73*, 337–341.

Iwaniec, D. M., Cook, E. M., Davidson, M. J., Berbés-Blázquez, M., Georgescu, M., Krayenhoff, E. S., … Grimm, N. B. (2020). The co-production of sustainable future scenarios. *Landscape and Urban Planning, 197*, 103744. https://doi.org/10.1016/j.landurbplan.2020.103744.

Keeler, B. L., Hamel, P., McPhearson, T., Hamann, M. H., Donahue, M. L., Meza Prado, K. A., … Wood, S. A. (2019). Social-ecological and technological factors moderate the value of urban nature. *Nature sustainability, 2*, 29–38. https://doi.org/10.1038/s41893-018-0202-1.

Kim, J.-H. (2003). Assessing practical significance of the proportional odds assumption. *Statistics & Probability Letters, 65*, 233–239. https://doi.org/10.1016/j.spl.2003.07.017.

Kuo, R. J., Huang, S. B. L., Zulvia, F. E., & Liao, T. W. (2018). Artificial bee colony-based support vector machines with feature selection and parameter optimization for rule extraction. *Knowledge and Information Systems, 55*, 253–274. https://doi.org/10.1007/s10115-017-1083-8.

Li, Y. (2012). MOMCMC: An efficient Monte Carlo method for multi-objective sampling over real parameter space. *Computers & Mathematcs with Applications, 64*, 3542–3556. https://doi.org/10.1016/j.camwa.2012.09.003.

Ma, S., Li, X., & Cai, Y. (2017). Delimiting the urban growth boundaries with a modified ant colony optimization model. *Computers, Environment and Urban Systems, 62*, 146–155. https://doi.org/10.1016/j.compenvurbsys.2016.11.004.

Metropolis, N., Rosenbluth, A. W., Rosenbluth, M. N., Teller, A. H., & Teller, E. (1953). Equation of state calculations by fast computing machines. *The Journal of Chemical Physics, 21*, 1087–1092. https://doi.org/10.1063/1.1699114.

Mileva, S., Suzana, D., Miloš, K., & Branislav, B. (2015). Modeling urban land use changes using support vector machines. *Transactions in GIS, 20*, 718–734. https://doi.org/10.1111/tgis.12174.

Montgomery, D. C., & Runger, G. C. (2003). *Applied statistics and probability for engineers* (Fourth. ed.). New York: John Wiley & Sons.

Mustafa, A., Heppenstall, A., Omrani, H., Saadi, I., Cools, M., & Teller, J. (2018). Modelling built-up expansion and densification with multinomial logistic regression, cellular automata and genetic algorithm. *Computers, Environment and Urban Systems, 67*, 147–156. https://doi.org/10.1016/j.compenvurbsys.2017.09.009.

Mustafa, A., Rienow, A., Saadi, I., Cools, M., & Teller, J. (2018). Comparing support vector machines with logistic regression for calibrating cellular automata land use change models. *European Journal of Remote Sensing*. https://doi.org/10.1080/22797254.2018.1442179.

Mustafa, A., Rompaey, A. V., Cools, M., Saadi, I., & Teller, J. (2018). Addressing the determinants of built-up expansion and densification processes at the regional scale. *Urban Studies, 55*, 3279–3298. https://doi.org/10.1177/0042098017749176.

Omrani, H., Parmentier, B., Helbich, M., & Pijanowski, B. (2019). The land transformation model-cluster framework: Applying k-means and the Spark computing environment for large scale land change analytics. *Environmental Modelling and Software, 111*, 182–191. https://doi.org/10.1016/j.envsoft.2018.10.004.

Puertas, O. L., Henríquez, C., & Meza, F. J. (2014). Assessing spatial dynamics of urban growth using an integrated land use model. Application in Santiago Metropolitan Area, 2010–2045. *Land Use Policy, 38*, 415–425. https://doi.org/10.1016/j.landusepol.2013.11.024.

Rienow, A., & Goetzke, R. (2015). Supporting SLEUTH – Enhancing a cellular automaton with support vector machines for urban growth modeling. *Computers, Environment and Urban Systems, 49*, 66–81. https://doi.org/10.1016/j.compenvurbsys.2014.05.001.

Scott, S. L., Blocker, A. W., Bonassi, F. V., Chipman, H. A., George, E. I., & McCulloch, R. E. (2016). Bayes and big data: The consensus Monte Carlo algorithm. *International Journal of Management Science and Engineering, 11*, 78–88. https://doi.org/10.1080/17509653.2016.1142191.

Strid, I. (2010). Efficient parallelisation of Metropolis–Hastings algorithms using a prefetching approach. *Computational Statistics & Data Analysis, The Fifth Special Issue on Computational Econometrics, 54*, 2814–2835. https://doi.org/10.1016/j.csda.2009.11.019.

Vermeiren, K., Vanmaercke, M., Beckers, J., & Van Rompaey, A. (2016). ASSURE: A model for the simulation of urban expansion and intra-urban social segregation. *International Journal of Geographical Information Science, 30*, 2377–2400. https://doi.org/10.1080/13658816.2016.1177641.

Vrugt, J. A., Gupta, H. V., Bastidas, L. A., Bouten, W., & Sorooshian, S. (2003). Effective and efficient algorithm for multiobjective optimization of hydrologic models. *Water Resources Research, 39*. https://doi.org/10.1029/2002WR001746.

White, R., & Engelen, G. (2000). High-resolution integrated modelling of the spatial dynamics of urban and regional systems. *Computers, Environment and Urban Systems, 24*, 383–400. https://doi.org/10.1016/S0198-9715(00)00012-0.

Xia, M., Zhang, Y., Zhang, Z., Liu, J., Ou, W., & Zou, W. (2020). Modeling agricultural land use change in a rapid urbanizing town: Linking the decisions of government, peasant households and enterprises. *Land Use Policy, 90*, 104266. https://doi.org/10.1016/j.landusepol.2019.104266.

XIU, Z. W. (2000). *Mathematical Foundation of Genetic Algorithms, 1* (edition. ed.). Xi'an Jiaotong University Press.

Yang, J., Tang, G., Cao, M., & Zhu, R. (2013). An intelligent method to discover transition rules for cellular automata using bee colony optimisation. *International Journal of Geographical Information Science, 27*, 1849–1864. https://doi.org/10.1080/13658816.2013.823498.

Yang, L., Jin, S., Danielson, P., Homer, C., Gass, L., Bender, S. M., … Xian, G. (2018). A new generation of the United States National Land Cover Database: Requirements, research priorities, design, and implementation strategies. *ISPRS Journal of Photogrammetry and Remote Sensing, 146*, 108–123. https://doi.org/10.1016/j.isprsjprs.2018.09.006.